Influence of Anisotropic Ion Heating on Confinement of the Tandem Mirror

K. Ishii 1), T. Goto 1), A. Itakura 1), I. Katanuma 1), Y. Katsuki 1), T.Saito 1), T. Tamano 1), A. Mase 2)

1) Plasma Research Center, University of Tsukuba, Tsukuba, Japan
2) Advanced Science and Technology Center for Cooperative Research, Kyushu University, Kasuga, Japan

e-mail: ishii@prc.tsukuba.ac.jp

Abstract. Ion transport in the velocity space due to the Alfvén ion-cyclotron (AIC) fluctuation was investigated using a developed diagnostic device ELECA (end-loss energy component analyzer) in the tandem mirror. The AIC waves are excited spontaneously in the central cell by carrying out anisotropic ion heating with injection of the ion-cyclotron range of frequency (ICRF) wave. Hump structure was observed on the energy distribution function of the end-loss ions, and was correlated with the excitation of the AIC wave. A remarkable feature is that trapped ions with characteristic energy flow selectively into the loss region so as to cause the hump structure which appears in the energy region (1.0 – 5.0) keV. The AIC waves enhance the ion diffusion from the trapped region to the loss region in the velocity space, and decrease the confinement. However, it was found that the hump structure decreased in the high potential mode and the high confining potential more than 3 kV could confine a large mount of loss energy flux due to the AIC fluctuations because of the existence of the upper limit of the hump energy, even in strong excitation of the AIC wave caused by high anisotropy.

1. Introduction

Loss regions exist necessarily in velocity space of the plasma in open systems. In order to improve axial confinement of the plasma in the tandem mirror, electrostatic potentials are created on both sides of the plasma, and the hyperboloidal loss boundaries in the velocity space have been shifted in the direction of higher energy along a velocity component axis parallel to the magnetic field. To achieve controlled thermonuclear fusion the plasma must be heated effectively, usually ions are heated anisotropically and at the same time fluctuations are excited in the plasma due to the anisotropic ion temperature. In the hot ion mode operation of the tandem mirror, spontaneous excitation of Alfvén ion-cyclotron (AIC) fluctuations was observed in the central cell plasma with anisotropic ion temperature [1]. It was pointed out that the AIC fluctuations enhanced the transport of the ions in the velocity space [2]. In the tandem mirror, the AIC fluctuations increase the ions which are scattered into the loss region from the trapped region across the hyperboloidal loss boundary. We summarize the ion transport phenomenon caused by the AIC fluctuations without ECRH using a newly-developed diagnostics of an end-loss energy component analyzer (ELECA) [3], and apply to the plasma with the plug potentials.

2. Experimental Apparatus

The tandem mirror GAMMA 10 was designed to be an effective axisymmetrized tandem mirror [4]. The machine is composed of two axisymmetric end mirror cells, two non-axisymmetric anchor cells and an axisymmetric central cell. In order to produce the plasma and heat the ions, ion-cyclotron range of frequency (ICRF) waves (RF1: 10 MHz, RF2: 6.36 MHz, RF3: 63 MHz) are injected into the target plasma in the central cell. Electrostatic plug potentials are created by carrying out electron cyclotron resonance heating (ECRH) at both the plug regions. Creation of axisymmetric potential profile at the plug cell is required to decrease radial transport of the tandem mirror plasma. The injection angle of the microwave was adjusted so as to axisymmetrize the potential profile, and was confirmed by measuring two dimensional potential profiles over the cross section of the plasma column at the thermal barrier cell using an improved gold neutral beam probe (GNBP) [5]. Coaxially segmented end plates are inserted in front of end walls to control the radial potential profile of the plasma. In the high confining potential mode of this experiment, a net of mesh made of stainless steel is installed in front of the central end plate, and biased negatively so as to create higher plug potentials by preventing the secondary electron emitted from the end plate

flowing into the plug region and to flatten the radial potential profile of the plasma. The plug potential is measured by the ELECA, and three sets of GNBPs are used to measure the electrostatic potentials of the barrier cell, the inner mirror throat of the plug/barrier cell and the central cell. The axial profile of the magnetic field strength is shown in Fig.1 with the locations of the heating systems, the ELECA device and the GNBP systems.

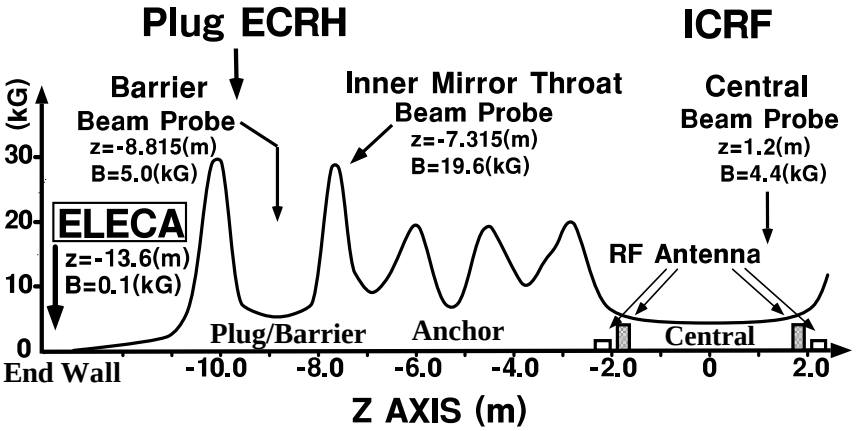

Fig.1 Axial profile of the magnetic field strength and locations of the heating systems and the potential diagnostic systems.

3. Measurements of End-Loss Ion and Electrostatic Potentials

A bird's eye view of the ELECA is shown in Fig.2. The energy distribution function $f_{\varepsilon}(\varepsilon)$, velocity distribution function $f(v_{\parallel}, v_{\perp})$ and energy flux $F_{\varepsilon\,\mathrm{loss}}$ of the end-loss ions are described as

$$f_{\varepsilon}(\varepsilon) = \frac{\sqrt{m}}{\sqrt{2}\, e \delta s\, R_A \sqrt{\varepsilon^3}} \sum_{z_a=0}^{z_{max}} 2\Delta I_s(\varepsilon, z_a)$$

for without an entrance slit,

$$f(v_{\perp}, v_{\parallel}) = \frac{m^2\, l_{es}\, l_{mp}\, \Delta I(\varepsilon, z_a)}{2 e \delta s\, R_A\, \delta\omega_{es}\, \varepsilon^2\, \Delta z_a}$$

for with an entrance slit, and

$$F_{\varepsilon\,\mathrm{loss}} = \frac{\sqrt{2}}{\sqrt{m}} \int d\varepsilon \sqrt{\varepsilon^3}\, f_{\varepsilon}(\varepsilon) \quad ,$$

where m is the ion mass, e is the unit charge, δs is the area of the small entrance aperture, R_A is the resolution of the ELECA, z_a is the position of the ion detector, z_{max} is the z_a coordinate of the small detector which detects the ion with the maximum pitch angle, $\Delta I_s(\varepsilon, z_a)$ is the ion current which enters the small detector located between z_a and $z_a + \Delta z_a$, $\delta\omega_{es}$ is slit width, l_{es} is slit distance, and l_{mp} is main path. The improved GNBP system at the barrier region is shown in Fig.3. The gold negative ion beam is neutralized by passing through a hydrogen gas box with high efficiency, and high neutral beam current is obtained. The merits are that the GNBP is available for a wide range of plasma density and the trajectories are simple under the irregular leakage magnetic field. By sweeping quickly both the energy and deflection angle of the beam, we measured two dimensional potential profiles and found the adequate injection condition of the microwave to create axisymmetric potential profiles.

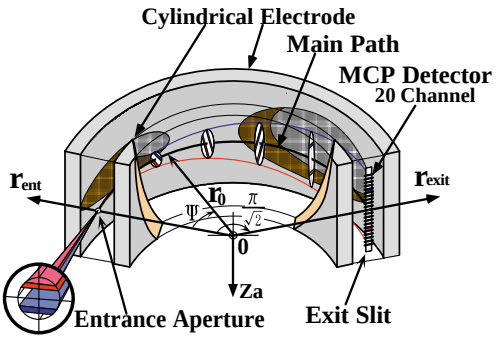

Fig2. Bird's eye view of the ELECA. The entrance slit is installed in front of the entrance aperture.

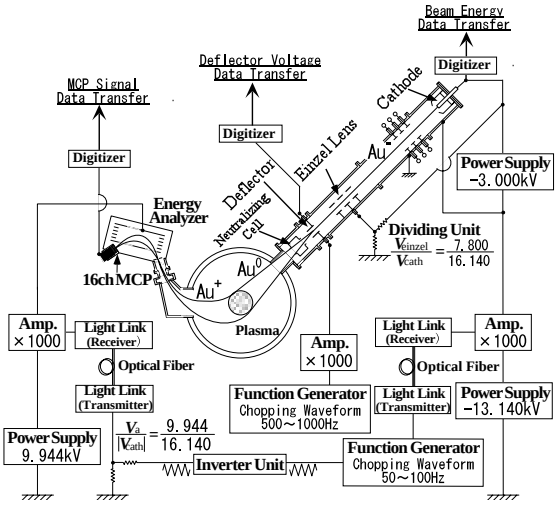

Fig.3 GNBP system at the barrier region. The energy is swept from 10 keV to 25 keV.

4. Hump Structure on Distribution Function of End-Loss Ions

We summarize the ion transport phenomenon caused by the AIC fluctuations without ECRH and apply to the plasma with the plug potentials.

When the ions were heated by the ICRF wave (RF2), the temperature anisotropy defined as the ratio of the perpendicular ion temperature to the parallel often exceeded 10 in the central cell. The strongly excited AIC fluctuations were also observed in the central cell by using magnetic probes and microwave reflectometers.
On the other hand, a hump structure was observed on the energy distribution function of the end-loss ions as shown in Figs. 4 (a), 4(b). In order to investigate the ion transport from a microscopic viewpoint in the velocity space, the pitch angles of the end-loss ions were also resolved as shown in Fig.4(c). Scattering with large pitch angles were observed in the hump region which was different from the Coulomb collision and indicated the characteristic of wave particle interaction. A remarkable feature of the hump structure is that trapped ions with characteristic energy flow selectively into the loss region so as to cause the hump structure which appears in the energy range of (~1.0-5.0) keV, and the excitation of the AIC fluctuations correlates strongly with the existence of the hump structure [6]. The mechanism of the hump structure was considered at the point of the interaction with the AIC waves. The lower and upper sides of the hump energy were explained from a viewpoint of ion trajectories in the ε-μ space induced by the cyclotron harmonic resonance due to small amplitude electromagnetic waves, where μ is the magnetic moment. Using the characteristic equation for the fundamental cyclotron resonance, the parallel velocity component $v_{\parallel 0}$ and the perpendicular velocity component $v_{\perp 0}$ at the midplane of the central cell, the equation is described as

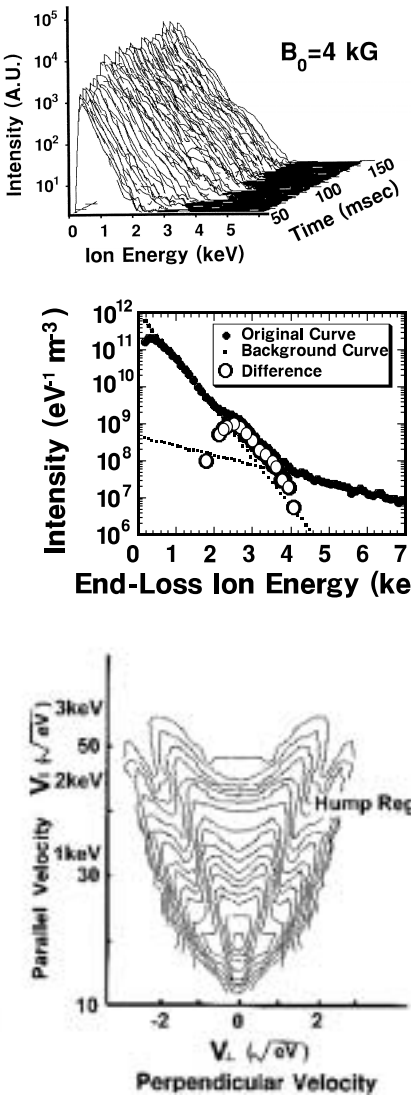

Fig.4(a) Time evolution of energy distribution function. The hump structure was observed. (b) An example of the hump structure. Open circles mean the enhanced ion loss. (c) Velocity distribution function. Contour lines are plotted on a logarithmic scale. Double loss boundaries correspond to the inner and outer mirror throat loss boundaries.

$$\mu = \left(\frac{\Omega_0}{B_0\,\omega}\right)\varepsilon - C\,, \qquad C \geq 0\,, \qquad \frac{v_{\parallel 0}^2}{(\frac{\Omega_0}{\omega} - 1)} + \frac{v_{\perp 0}^2}{(\frac{\Omega_0}{\omega})} = \frac{2\,B_0\,C}{(\frac{\Omega_0}{\omega})(\frac{\Omega_0}{\omega} - 1)m}\,.$$

where $\Omega_0 = eB_0/m$, B_0 is the magnetic field at the midplane, ω is the angular frequency of the wave, and C is constant [7]. The angular frequency of the excited AIC wave is lower than the ion-cyclotron angular frequency at the midplane of the central cell, therefore the curves become ellipses as shown in Fig.5. The ion-cyclotron resonance condition is described as $\omega - k_\parallel v_\parallel = \Omega$, where $k_\parallel$ is the parallel component of the wave number, $v_\parallel$ is the parallel velocity

component, and Ω is the ion-cyclotron angular frequency. As the end-loss ions are detected at the position of z = -13.6 m, $v_{\parallel}$ is negative and $k_{\parallel}$ is positive. Because of $\Omega \geq \Omega_0$, the low energy of the resonant particle is restricted to $(m/2)\{(\Omega_0 - \omega)/k_{\parallel}\}^2$.

The upper limit of the hump energy is restricted by the ion-cyclotron angular frequency corresponding to the magnetic field with a steep gradient. In the region of the magnetic field with a steep gradient, the ions with large perpendicular velocity components are reflected so as to decrease β value, and the ions are not affected by the wave effectively because the cyclotron frequency varies rapidly and the intensity of the wave decreases. As the frequency and the parallel wave number of the spontaneously excited AIC wave are changed with the temperature anisotropy and β value, the energy of the hump structure is spread over the characteristic range of energy. We directly measured the parallel wave number and the angular frequency of the AIC wave by use of the magnetic probes [8], and simultaneously measured the hump energy on the energy distribution function of the end-loss ions.

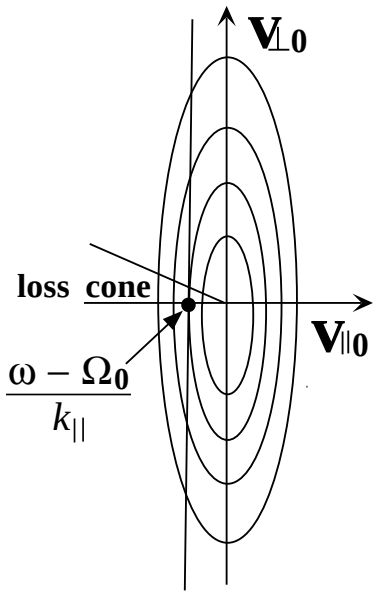

Fig.5 Heating characteristic curve. The curves are ellipses.

The resonance energies of 1.6 keV and 2.5 keV were obtained for $\omega = 2\pi \times 7.11$ MHz, $k_{\parallel} = 8.8$ m^{-1} and $\omega = 2\pi \times 7.07$ MHz, $k_{\parallel} = 7.0$ m^{-1}, respectively.

The hump energy is in good agreement with the estimated energy. Here we define an enhancement factor $g_{\text{ehf (FWHM)}}$ as a ratio of the energy flux $F_{\varepsilon\,\text{loss(FWHM)}}$ of the original curve inside of the full width at half maximum (FWHM) of the hump to the background energy flux $F_{\varepsilon\,\text{loss(FWHM)}}$(background) as follows,

$$g_{\text{ehf (FWHM)}} = \frac{F_{\varepsilon\,\text{loss (FWHM)}}}{F_{\varepsilon\,\text{loss (FWHM)}}\,(\text{background})}\ , \qquad F_{\varepsilon\,\text{loss (FWHM)}} = \frac{\sqrt{2}}{\sqrt{m}} \int_{\text{inside-of -FWHM}} d\varepsilon \sqrt{\varepsilon^3}\ f_{\varepsilon}(\varepsilon).$$

The background curve, which is fitted well without the hump, is estimated approximately as a summed up line of two types of straight lines on the lower and higher sides. The factor grows easily up to 4 for the peak energy of ~2.5 keV without the confining potential. As the confining potential approaches the hump energy, the loss flow due to the hump structure becomes effective. Thus we investigated the influence in the high confining potential mode.

The experiment was carried out by controlling the end-plate potential with the resistors and applying the mesh bias only in the central part in order to avoid inflow of the secondary electrons emitted from the end-plate and to heat the plug electron effectively. The potential configuration of the tandem mirror was confirmed by measuring the axial profile of the electrostatic potential.

We measured the plug potential (Φ_P) with ~1 kV for the axisymmetrized microwave injection with the power of 130 kW, and also measured the potential at the inner mirror throat and confirmed possibility of the effective thermal barrier region.

By creation of the plug potential, the double loss boundaries appeared in the velocity distribution function of the end-loss ions were changed to a single loss boundary, and also the hump structure decreased in the high potential mode.

The enhancement factor had a tendency not to exceed the value of 3 as shown in Fig. 6(b).

This is caused by the relaxation of the anisotropy

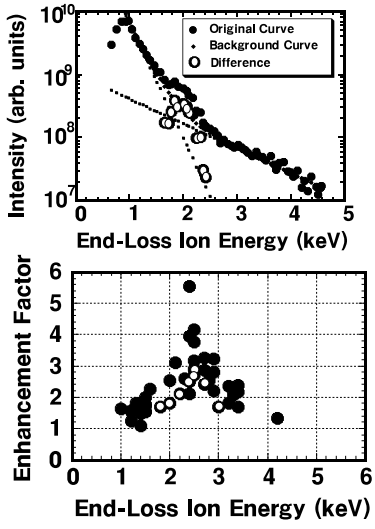

Fig.6(a) Energy distribution function. (b) Energy dependence of enhancement factor. Open circles indicate the case with ECRH.

due to the ECRH. Figure 6(a) is an example of the energy distribution function with a hump structure ($g_{ehf(FWHM)}$ ~2) and the plug potential (Φ_P) with ~1 kV.

6. Summary

Ions are heated anisotropically by carrying out ICRF heating in the central cell. The AIC fluctuations are spontaneously excited in the central cell due to the anisotropic ion heating, and enhance the ion diffusion from the trapped region to the loss region so as to produce the hump structure on the energy distribution function of the end-loss ions. The enhancement factor corresponding to the energy more than 2.0 keV grows up to about 4 easily. However, the hump structure decreases in the high potential mode and the high confining potential more than 3 kV can confine a large amount of loss energy flux due to the AIC fluctuations because of the existence of the upper limit of the hump energy, even in strong excitation of the AIC wave caused by the high anisotropy.

Acknowledgements

The authors are deeply grateful to the members of GAMMA 10 for their collaboration in the experiments and discussions.

References

[1] M. ICHIMURA, et al., Plasma Phys. Controlled Fusion **34**, (1992) 1889.
[2]T. Tajima and J. M. Dawson, Nucl. Fusion **20**, (1980) 1129.
[3] K. ISHII, et al., J. Phys. Soc. Jpn. **66**, (1997) 2224.
[4] M. INUTAKE, et al., Phys. Rev. Lett. **55** (1985) 939.
[5] N. KIKUNO, et al., Rev. Sci. Instrum. **70**, (1999) 4251.
[6] K. ISHII, et al., Phys. Rev. Lett. **83**, No.17 (1999) 3438.
[7] T. D. ROGNLIEN, Phys. Fluids **26** (1983) 1545.
[8] A. KUMAGAI, et al., Jpn. J. Appl. Phys. **36**, (1997) 6978.